

We are IntechOpen, the world's leading publisher of Open Access books Built by scientists, for scientists

6,900

Open access books available

185,000

International authors and editors

200M

Downloads

Our authors are among the

154

Countries delivered to

TOP 1%

most cited scientists

12.2%

Contributors from top 500 universities



WEB OF SCIENCE™

Selection of our books indexed in the Book Citation Index
in Web of Science™ Core Collection (BKCI)

Interested in publishing with us?
Contact book.department@intechopen.com

Numbers displayed above are based on latest data collected.
For more information visit www.intechopen.com



Non-Destructive Testing of Low-Velocity Impacted Composite Material Laminates through Ultrasonic Inspection Methods

Tiziana Segreto, Roberto Teti and
Valentina Lopresto

Additional information is available at the end of the chapter

<http://dx.doi.org/10.5772/intechopen.80573>

Abstract

Low-velocity impact damages in composite material laminates, such as matrix cracks, delaminations and fibre breakage, usually develop inside the material and can be difficult to detect. As these flaws downgrade the structural integrity of the composite, the thorough damage evaluation is essential to assess the impact damage criticality. This chapter focuses on the ultrasonic non-destructive inspection of low-velocity impacted composite laminates for damage estimation and assessment. The impact damage generation mechanisms are described and characterised. Ultrasonic testing methods and their defect detection capabilities are illustrated. Recent research studies on ultrasonic non-destructive evaluation of low-velocity impacted composite materials are presented and discussed.

Keywords: composite materials, low-velocity impact, non-destructive testing, ultrasonic inspection

1. Introduction

Low-velocity impact is one of the most subtle threats to composite materials integrity. Due to the weak bonds between the plies, even small energies imparted by out-of-plane loads can result in hardly detectable damages, such as matrix cracks, delamination and fibre breakage, causing considerable stiffness and strength losses in tension and, especially, in compression and severely reducing the material structural integrity. Generally, the main observable

damage affecting a laminate subjected to low-velocity impact is delamination, mainly responsible for compression strength decay. For this reason, diverse research works have been devoted to the mechanisms of delamination initiation and growth [1–6]. During impact, more than one delamination in the thickness direction generally develops in a composite laminate, depending on the impact energy and the laminate stacking sequence. Hence, it is crucial to understand the mechanisms of impact damage onset and growth in composite laminates.

To date, non-destructive testing (NDT) techniques play a fundamental role in diverse industrial areas (such as aerospace, automotive, naval and sporting goods, etc.) for the detection of defects in composite material components in order to ensure their integrity during both the manufacturing phase and the service life [7]. Many types of NDT methods are used for flaw analysis, including ultrasonic inspection, X-ray, acoustography, shearography, acoustic emission, etc. [8].

Ultrasonic testing is the most widely utilised NDT procedure for the detection of flaws in composite materials, allowing the identification and characterisation of internal and external damages without cutting apart or otherwise altering the composite material. The main advantages of UT NDT include [9]: high penetration capacity, which allows to inspect parts of large size; high sensitivity, permitting to detect extremely small defects; only one surface of the part needs to be accessible for UT testing and no hazards exist for the operator or the test materials. The disadvantages of UT NDT comprise: need for expert operators; difficulty in inspecting rough surfaces with irregular or too small shapes; need for a coupling medium between the UT probe and the test part and reference standards are required for both instrument calibration and defect characterisation. In this chapter, the non-destructive characterisation and assessment of low-velocity impact damage in composite material laminates is investigated through UT inspection. A description of low-velocity impact damage generation and development in composite materials is presented in Section 2. Section 3 gives an overview of the UT testing methods, describing the basic principles, the UT inspection systems, the defect identification capabilities and the UT data representation; moreover, the UT NDT techniques applied to composite materials are illustrated. In the last section, the research studies of the last several years on the detection of defects generated in low-velocity impacted composite materials are presented and discussed.

2. Impact damage in composite materials

By considering that for many composite materials applications, such as body panels of cars, trucks, rail vehicles and aircraft fuselage, the designer of the composite structure must ensure the prevention of penetration by foreign objects of known mass and velocity. Accordingly, the knowledge of penetration energy becomes a critical issue. Moreover, the absorbed energy is a fundamental parameter in impact situations where it is necessary that the mechanical shock is not transferred to the human body, such as in motorcycle helmets and race car frames, with the aim to ensure the driver's safety in case of high-speed crashes. Accordingly, for these applications, laminated composites must be designed to absorb as much as possible the impact energy and to limit the decelerations on the human body.

Due to their brittleness and anisotropy, composite laminates are particularly sensitive to low-velocity impact damage caused by accidental loadings imparted during fabrication or

service. This has led to numerous studies concerning impact dynamics [10–12], mechanisms of failure initiation and propagation [12–15] and correlation between impact energy, damage and residual material properties [2, 9, 12, 16–18].

Delamination is the most important and crucial damage caused by dynamic loading conditions. Matrix cracking consists in cracks that develop in the resin rich areas between two adjacent composite layers. It has been observed that delamination occurs when a threshold energy is reached in presence of matrix cracking [19]. Even if there is a common agreement on the mechanisms of initiation and growth of this failure mode during an impact event, and several research studies are devoted to this topic [15, 20], a general approach to predict the damage mechanisms and interaction in order to prevent catastrophic failures, is absent. The complexity of the stresses in the vicinity of the point of impact complicates the analysis. In [21], it was shown that delamination growth is governed by interlaminar longitudinal shear stress (σ_{13}) and transverse in-plane stress (σ_{22}) in the layer below the delaminated interface and by the interlaminar transverse shear stress (σ_{23}) in the layer above the interface.

A critical aspect of impact damage is the fact that it is difficult to detect by visual inspection: a composite structure can be severely damaged without any external sign. The only external indication of an impact is indentation, that is, the plastic deformation of the laminate surface due to the contact, left by the impactor during the loading phase. This has led to the concept of “barely visible impact damage”, usually adopted in the design of aeronautical structures.

2.1. Experimental characterisation of impact damage

A thorough study of the behaviour of composite laminates subjected to dynamic loads, was carried out by [1–6, 12–14], with the aim to understand the complex mechanisms of damage initiation and propagation under low-velocity impact loading. Many parameters are involved in an impact event and the diverse induced damages, together with their interaction, are very complex to investigate. Moreover, there are instances where impact damage, though seriously present inside the material, is barely visible or not at all visible from the outside.

An extensive experimental testing campaign was carried out on different composite material systems by increasing the initial kinetic energy up to the complete material penetration [16]. This allowed the study of the initiation and the propagation of the complex failure modes related to impact damage. The starting point was the study of the load-deflection curves recorded during impact testing for all the different test conditions. From the curves, the relevant impact parameters were obtained: first failure load and energy, maximum load and energy, absorbed and penetration energy. The influence on the impact parameters, exercised by the composite system, the material constituents, the thickness and the laminate stacking sequence as well as the constraint conditions and the tup diameter were evaluated. Destructive and non-destructive testing were applied to investigate the failure modes, and the observed damage was correlated to the relative energies and the other relevant parameters.

Indentation was found to be a function of the impact energy on the basis of the perforation energy. The latter represents the minimum kinetic energy necessary to completely penetrate

the laminate and is evaluated as the area under the complete load-displacement curve at penetration [22]. This is a fundamental parameter to be known in order to gather information about the impact energy that causes the loss of material mechanical properties [16, 23].

2.2. Load-displacement curve analysis

The load-displacement curve recorded during experimental impact tests is a fundamental tool to obtain information about the impact response and behaviour of composite material samples or structures under service conditions. Some characteristic points on the recorded curve are correlated with the evolution of the impact damage inside the material. In correspondence of these points, the first failure load and energy, the maximum load and energy, the absorbed and the penetration energy, were calculated. The influence of the thickness, the laminate stacking sequence, the matrix type and content, the fibre type and orientations and the impact conditions (impactor tup, diameter of sample support and load speed) was clearly evidenced by comparing the load-displacement curves obtained under the different test conditions. The examination of the load-displacement curves evidence that, notwithstanding the differences in thickness, material composition and reinforcement architecture, there are typical features common to all composite laminates subjected to impact testing [24]. **Figure 1** shows a schematic view of a typical load-displacement curve with the characteristic points identified by arrows and letters ("a", "b", "c", "d", "e").

In **Figure 2**, four curves from low-velocity impact tests on carbon fibre reinforced polymer (CFRP) laminates with different thicknesses are overlapped: despite the thickness difference, common features can be clearly noted. Up to point "a", the curve shows no evidence of damage developing inside the material. A different behaviour between thin and thick laminates can be observed due to the increase of the initial laminate rigidity with increasing thickness (**Figure 2**). The thinner laminates display a clear non-linear response for very low displacement

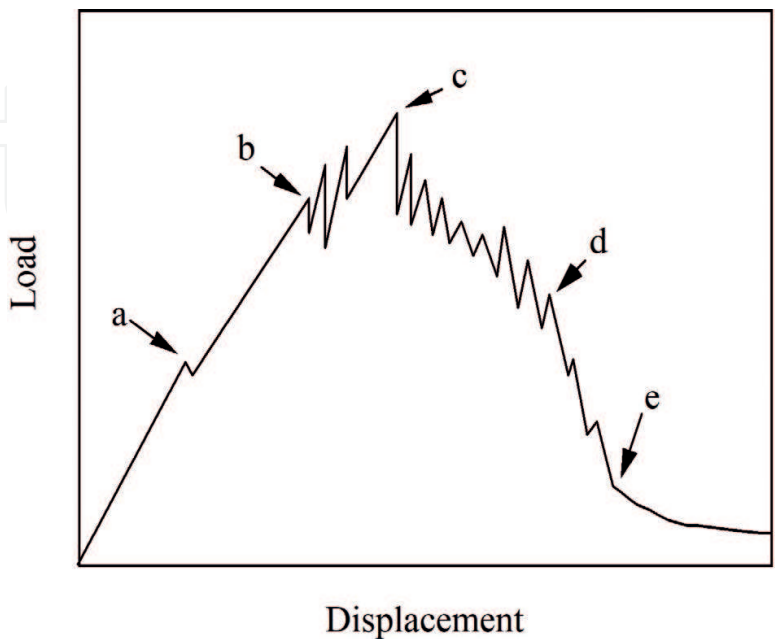


Figure 1. Schematic view of the impact load-displacement curve at penetration.

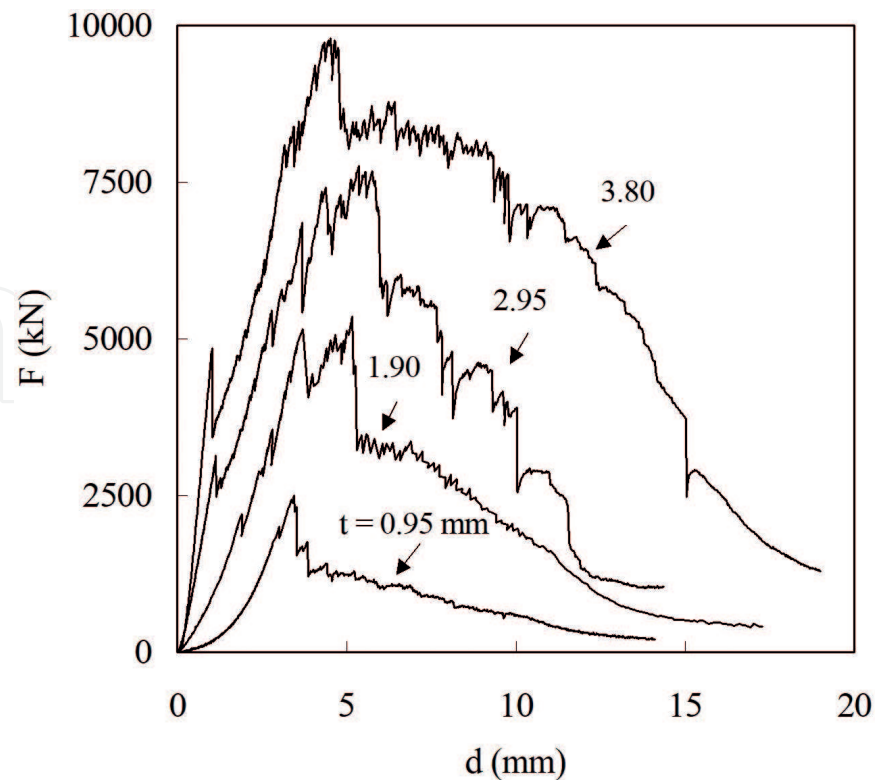


Figure 2. Load, F , versus displacement, d , curves for different CFRP laminate thickness, t .

values, due to the larger amount of displacement at low impact force in comparison with the thicker laminates [25]. At the end of the elastic phase, a load drop occurs, the more clearly when the material thickness is sufficiently high (point “a” in **Figure 1**). This behaviour is difficult to appreciate for the lowest thickness where the load remains substantially constant with increasing displacement or a different slope is evidenced. However, in both cases, a local rigidity variation happens, denoting damage in the laminate.

The successive load drop is an indication of fibre breakage and/or damage propagation in the form of matrix cracking, delamination, fibre breakage, fibre/matrix debonding and fibre pull out (point “b” on the curve). Matrix cracking in the resin pockets are the first type of damage developed during an impact [25] and the presence of matrix cracks does not affect the overall laminate stiffness [26]. However, matrix cracks represent the initiation point for delamination [4, 21] and fibre breakage which dramatically change the stiffness of the composite laminate [27]. All the energy exceeding the one necessary for these damage initiation phenomena is employed for damage propagation. After the first failure, the load increases again, although the laminate rigidity is reduced. Then, a series of load drops are noted, resulting in oscillations in the force-displacement curve, which correspond to extensive propagation of failures of fibres and in the resin through-the-thickness. In the range from points “b” to “d” (**Figure 1**), the different damages propagate through all the layers, until the complete perforation is achieved (point “d”). The slope of the load-displacement curve begins to rapidly decrease when composite material perforation occurs. The maximum force (point “c”) is generally achieved between points “b” and “d”, even for the thicker laminates (12 layers or more); point “b” is often found coincident with point “d”, which means that the first significant fibre failure frequently occurs at maximum force [24].

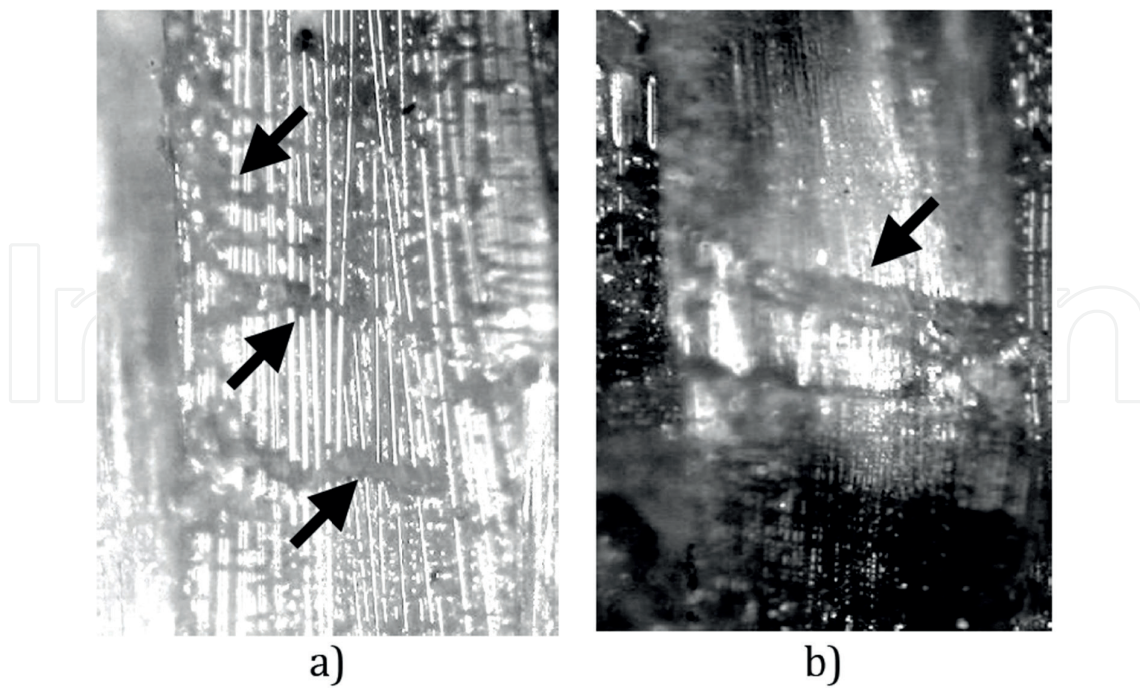


Figure 3. Fibre failures indicated by the black arrows.

In **Figure 3**, examples of fibre failures are shown. The decrease in contact load between points “d” and “e” corresponds to the penetration process. Finally, beyond point “e”, the contact load decreases slowly: the cylindrical body of the impactor slides through the penetrated sample. The penetration energy necessary to completely penetrate the laminate, given by the area under the load-displacement curve at penetration, is conventionally calculated at point “e”. Both **Figures 1** and **2** refer to impact test cases where complete perforation occurred. In case of non-perforating impacts, during the loading phase the maximum displacement is reached and then the displacement decreases during unloading (**Figure 4**). After the first load drop (arrows in **Figure 4**), the unloading part is different from the loading one since a fraction of the energy is stored in the material for damage formation.

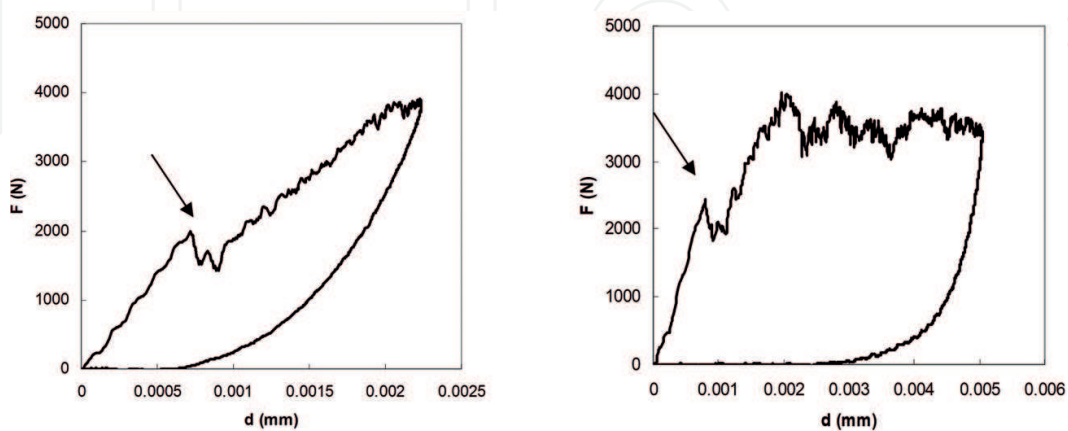


Figure 4. Load-displacement curves for a not penetrated CFRP laminate ($t = 3$ mm): (a) impact energy level $U = 5$ J; (b) impact energy level $U = 15$ J.

In [5], it was demonstrated that an interaction between matrix cracking and delamination initiation exists. Delamination propagation starting from intralaminar cracks was found mainly in thin laminates [5, 28] where the membrane contribution is important. In **Figure 5**, low (a) and high (b) magnification micrographs of dynamically loaded CFRP samples are reported showing matrix cracks and delamination starting from the cracks in the resin pocket and connected by intralaminar cracks [5].

As found in several research works by different authors [6, 21], the evolution of damage in a composite laminate subjected to a concentrated dynamic load is driven by intralaminar tensile and shear cracks occurring in the layers farther from and nearer to the contact point. From these cracks, delaminations were found to be generated at interfaces between differently oriented plies, mainly propagating in the direction of the fibres in the lower ply and extending the more sideways with respect to the contact point.

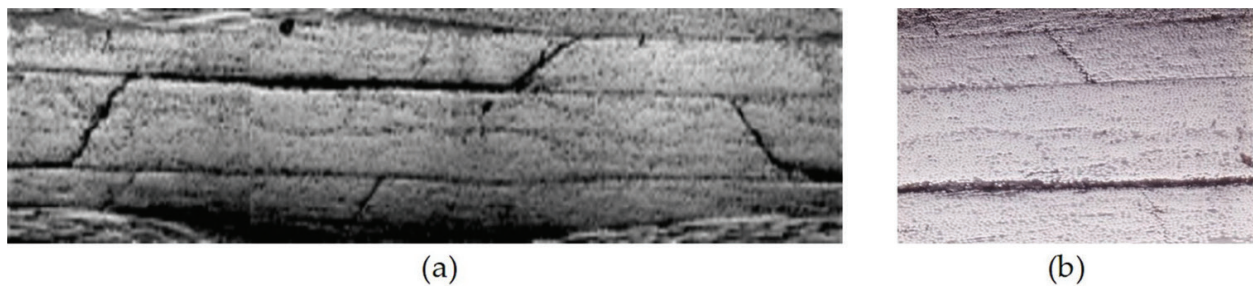


Figure 5. Low (a) and high (b) magnification micrographs of dynamically loaded CFRP laminate with thickness $t = 2$ mm.

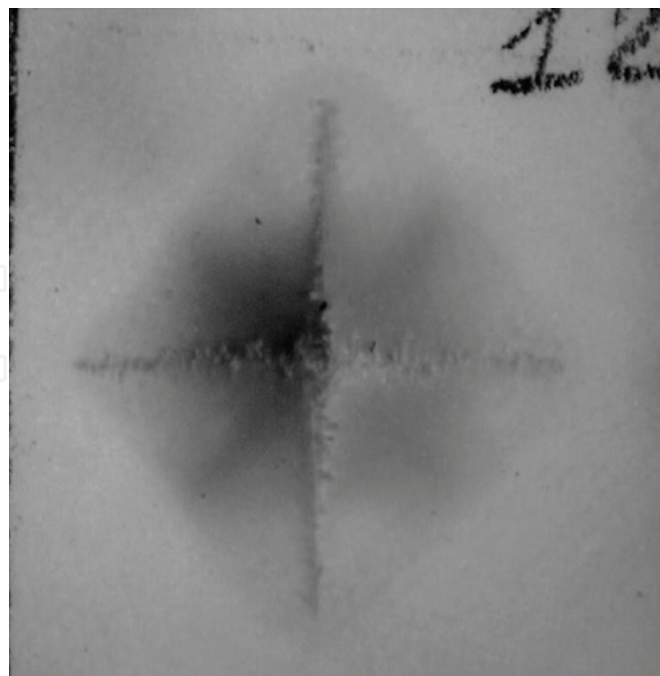


Figure 6. Typical damage zone after impact (back laminate surface). Laminate thickness $t = 1.92$ mm. Impact energy $U = 15.8$ J.

A different behaviour is noted for thin and for thick laminates. In thin laminates, bending stresses are more important whereas shear stresses predominate in thick laminates and delaminations without evidence of intralaminar cracks were found at mid-thickness.

In **Figure 6**, a typical impact damage, visually observed on to the back surface of the impacted laminate, is reported, where the classical visible diamond-shaped delaminated area has attained its maximum size. The delamination axes coincide with the warp-weft fibre directions of the surface fabric layer.

3. Ultrasonic non-destructive testing

During World War I, underwater detection systems using high-frequency acoustic waves and quartz resonators for submarine detection were developed by Langevin [29] as a consequence to the tragic sinking of the Titanic in 1912. In 1928, Sergei Y. Sokolov proposed the use of a through-transmission UT technique for flaw detection in metals [30]. Mulhauser firstly patented an UT device employing separate transmitter and receiver transducers to detect flaws in solids [29]. In 1940, Firestone was the first to realise the UT reflection or pulse-echo technique [31]. In 1948, extensive study of UT medical imaging started in the United States and Japan. One of the first UT testing apparatuses using piezoelectric crystal transducers for the detection of defects was patented by McNulty in 1962. This apparatus was capable of isolating defect signals from high level noise signals and providing an alarm upon occurrence of a defect signal [32]. Since those times, technology improvements led to remarkably enhanced UT non-destructive testing (NDT) allowing to detect surface, subsurface and internal flaws (cracks, delaminations, cavities, pores, inclusions and fractures) in diverse types of materials (metals, composite materials and plastics) [33]. In the manufacturing industries, UT NDT techniques are widely applied for the quality control of components and structures as well as for the characterisation of materials.

3.1. Basic principles

UT NDT is based on the measurement of the energy variations associated with mechanical waves, with frequencies ranging between 50 kHz and 25 MHz, generated by a piezoelectric transducer. The UT beams are introduced into the material by a coupling medium (oil, grease and water) and the variations of the reflected and/or transmitted UT energy are used to identify defects within the material which represent discontinuities in the UT path. When an atomic or molecular particle is displaced from its equilibrium position due to UT waves propagation in the material, the internal (interatomic or intermolecular) forces tend to bring it back to its original position. The displacement of a particle causes the dislocation of those placed in the neighbourhood, and thus the propagation of the UT waves in all the material is determined [8, 34].

In **Figure 7**, the basic parameters of a continuous UT wave are shown. The distance between two consecutive peaks of an UT wave is the wavelength, λ , while the number of UT oscillations per unit time is the frequency, f . The time required to complete a full cycle is the period T . The relation between frequency and period in a continuous wave is given by:

$$f = \frac{1}{T} \quad (1)$$

UT velocity, v , in a perfectly elastic material at a given temperature and pressure is constant. The relationship between v , f and λ is given by Eqs. (2) and (3).

$$\lambda = \frac{v}{f} \quad (2)$$

$$\lambda = vT \quad (3)$$

In UT NDT, the shorter wavelength resulting from an increase in frequency will usually provide for the capability to detect smaller discontinuities. As a general rule, a discontinuity must be larger than one-half the wavelength in order to be detected. Based on the particle displacement mode, UT waves are classified as longitudinal, shear, surface, and Lamb waves. Longitudinal waves are compressional waves where the particle motion is parallel to the propagation direction of the wave. Shear waves are present when the oscillation direction is perpendicular to the propagation direction. Surface (Rayleigh) waves have an elliptical particle motion and travel across the surface following the profile of the material. Plate (Lamb) waves have a complex vibration occurring in materials where the thickness is less than the wavelength of the UT waves introduced into it.

UT propagation velocity in a medium and UT wave attenuation (loss of amplitude and energy) depend on the medium itself. In solids, the velocity of longitudinal waves, V_L , is given by:

$$V_L = \sqrt{\frac{E(1-\nu)}{\rho(1+\nu)(1-2\nu)}} \quad (4)$$

where E = Young's modulus; ν = Poisson's ratio; ρ = density of the material.

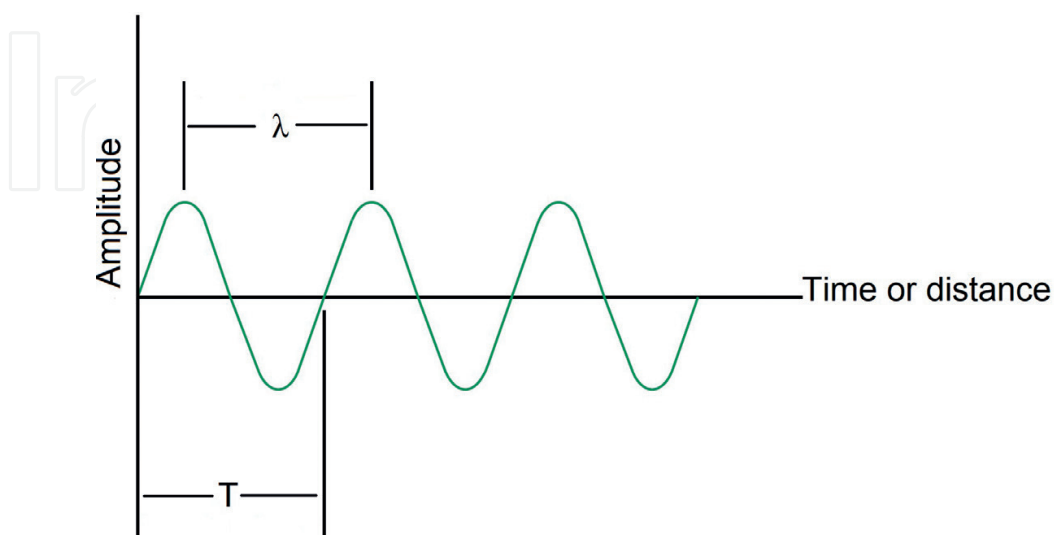


Figure 7. Basic parameters of an UT wave.

The speed of transverse (or shear) waves, V_T , depends on the shear deformation under shear stress (shear modulus) and the density of the medium, defined by the following formula:

$$V_T = \sqrt{\frac{G}{\rho}} \quad (5)$$

where G = shear modulus of elasticity.

In isotropic materials, the elastic constants are the same for all directions within the material. However, most materials are anisotropic and the elastic constants differ with each direction.

ASTM E494 - 15: "Standard Practice for Measuring Ultrasonic Velocity in Materials" covers a test procedure for measuring UT velocity in materials with conventional UT pulse-echo flaw detection equipment. In this practice, tables with longitudinal and shear velocities are reported for metal and ceramic materials [35].

UT attenuation is the decay rate of the UT wave as it propagates through a material. It is mainly due to absorption (conversion of sound energy into other forms of energy) and scattering (reflection of sound in directions other than the original propagation direction) phenomena. The amount of attenuation through a material is a critical parameter for the selection of the appropriate UT transducer for an application.

3.2. UT inspection system

The basic equipment of an UT inspection system consists of diverse functional units: pulser/receiver, transducer and display devices. A pulser/receiver is an electronic device generating short, high amplitude electric pulses which are converted by the transducer into high-frequency UT energy. The sound energy is introduced into the test material and propagates through the material in the form of UT waves. If there is a discontinuity (e.g. a crack) in the UT wave path, part of the energy is reflected back from the flaw surface. The reflected UT wave signal reaches the transducer which transforms it into an electrical signal that can be recorded and/or displayed on a screen [36].

The control functions associated with the pulser circuit include the pulse length or damping and the pulse energy, whereas the control functions in the receiver phase are related to the refinement, filtering and amplification of the return signals.

Selection of the appropriate UT transducer is the first significant step to be considered for UT inspection of a part. Two main categories of transducer are available: contact and immersion transducers. The first category refers to transducers utilised for direct contact inspections which are generally hand manipulated by a skilled operator. Diverse contact transducers are commercially available and their selection depends on the characteristics of the contact surface and the thickness of the part as well as on the aims of the UT inspection. The most common contact transducers are: flat contact, dual element and angle-beam transducers. Immersion transducers are designed to operate in a liquid environment and consequently are typically utilised inside a water tank or as part of a squirter system for UT NDT scanning applications. These transducers can be equipped with cylindrically or spherically focused lens. A focused transducer has the property to concentrate the sound energy onto a small area in order to improve sensitivity and axial resolution.

Two basic quantities are measured in UT testing: the time-of-flight (TOF) corresponding to the amount of time for the sound to travel through the sample, and the amplitude of the received signal. Based on velocity and round trip time-of-flight through the material, the material thickness, S , can be calculated as follows:

$$S = \frac{v t_s}{2} \quad (6)$$

where v = material sound velocity; t_s = time-of-flight.

Measurements of the relative change in UT signal amplitude can be used for sizing flaws or measuring the material attenuation properties.

3.3. Variables in UT inspection for defect detection

The major variables to be considered in UT NDT include the characteristics of the utilised UT waves and the proprieties of the part being inspected. UT equipment type and capability interact with these variables; often, different types of equipment need be selected to accomplish different inspection objectives. Generally, a compromise must be made between favourable and adverse effects to achieve an optimum balance and to overcome the limitations imposed by equipment and test material [37].

The frequency of the utilised UT waves affects the inspection capability in several ways:

- Sensitivity, or the capability of an UT inspection system to detect a very small discontinuity, is generally increased by using high frequencies (short wavelengths).
- Resolution, or the ability of the UT system to generate simultaneous and distinct indications from discontinuities located close to each other within the material or located close to the front surface of the part, is directly proportional to the frequency bandwidth and inversely related to the pulse length; resolution usually improves with increasing frequency.
- Penetration, or the maximum depth in a material from which useful indications can be detected, is reduced by the use of high frequencies; this effect is most pronounced in the inspection of metals with coarse grain structure or inhomogeneous materials, such as composites, due to the resultant scattering of the UT waves.
- Beam spread, or the divergence of an UT beam from its central axis, is also affected by frequency: as frequency decreases, the shape of an UT beam increasingly departs from the ideal of zero beam spread. This characteristic is observed at almost all frequencies used in UT inspection. Other factors, such as transducer diameter and the use of focusing lens, also affect beam spread.

Sensitivity, resolution, penetration and beam spread are largely determined by the selection of the transducer and are only slightly modified by changes in other test variables.

3.4. UT inspection methods and data representation

A first difference between UT inspection techniques can be made with reference to the transducer or probe position [34, 36, 37]:

- Contact technique, where the probe is placed directly on the surface of the part to be examined.
- Immersion technique, where the probe is immersed in a liquid substance that separates it from the part surface.

The main operating techniques of UT NDT are the through-transmission method and the pulse-echo (or reflection) method.

In the through-transmission technique, two probes, positioned at opposite sides with respect to the part, are used: one probe transmits the UT beam into the part and the other probe receives it. A defect, reflecting a part of the incident beam, causes a decrease in the UT energy detected by the receiving probe. The presence of the defect is highlighted by comparing the received signal with a reference signal obtained from a standard, flaw-less sample. In this technique, two opposite surfaces of the part under examination must be accessible to the transducers.

The pulse-echo technique is based on the property of the UT beam to be reflected whenever it encounters a discontinuity or a defect in its path. The amount of reflected energy highly depends on the reflecting surface size, that is, on the dimensions of the encountered discontinuity perpendicularly to the UT beam propagation direction. To perform the test, it is sufficient that only one surface of the part is accessible, since a single probe is used to send the incident UT beam and, at the same time, receive the reflected UT signal. In **Figure 8**, the typical UT waveform generated during UT pulse-echo inspection of a defective part is shown. The UT waveform enters the material and a first echo, called interface or front echo, is visualised. The back echo corresponds to the final (last) surface of the part under examination. If a discontinuity is encountered inside the material, a defect echo is visualised between the front and the back echoes.

Pulse-echo UT inspection can be accomplished with longitudinal, shear, surface or Lamb waves. Straight-beam or angle-beam techniques can be used, depending on the part shape and the inspection objectives. The detected UT data can be analysed to obtain the required information on defect characteristics, such as type, size, location and orientation.

Diverse representations of UT data are available. The most common formats utilised are: A-scan, B-scan, C-scan, D-scan and FV-scan [8, 9, 34, 36, 37].

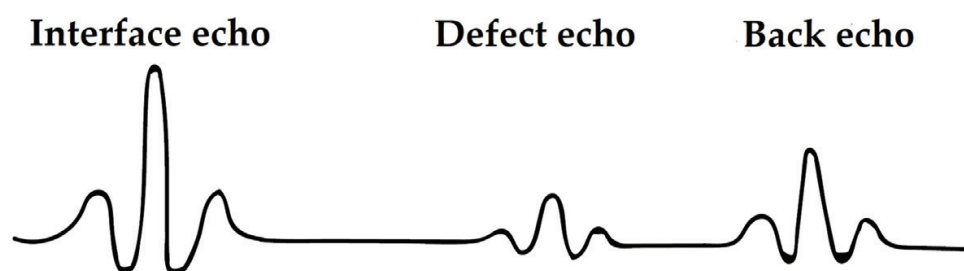


Figure 8. UT waveform generated during UT pulse-echo inspection of a defective part.

- A-scan. It provides a quantitative display of UT signal amplitudes (y axis) and time-of-flight information (x axis) obtained by UT material interrogation at a single point on the part surface. The A-scan can be used to analyse the type, size and location (chiefly depth) of flaws. A discontinuity in the material is indicated by a peak (echo) the distance of which from the zero of the time axis is proportional to the path that the UT beam performs before encountering the discontinuity itself. The amplitude of this defect peak is proportional to the acoustic energy reflected by the discontinuity.
- B-scan. This format provides a quantitative display of time-of-flight data reported along the y axis obtained during a linear scan (x axis) of the part. A B-scan provides information about the part thickness and the depth of a defect for a single plane that normally intersects the part arranged along the scan direction.
- C-scan. A semi-quantitative or quantitative display of UT signal amplitudes obtained over an area of the part surface is represented using a C-scan. The information can be used to map out the position of flaws in an UT image representing the plan view of the part. A C-scan format also records time-of-flight data, which can be converted and displayed by image processing techniques to provide information on flaw depth.
- D-scan. It is similar to a C-scan, but in this case the time-of-flight data obtained over an area of the part is utilised for UT image generation instead of the signal amplitude data.
- FV-scan. Full volume scan (FV-scan), or volumetric scan, is based on the detection and storage of the entire UT waveform in the propagation direction (z-direction) during x-y scanning of the part surface. FV-scan provides for the 2½ D representation of the material internal structure, based on the generation of C-scans at any depth along the z-axis for any portion of the material thickness.

3.5. UT inspection of composite materials

Due to the non-homogeneous and anisotropic nature of composites materials, the frequency range utilised in UT NDT of composites is markedly reduced due to the high damping and attenuation of the high-frequency signals. Usually, the employed frequency in industrial applications is 5 MHz or less, limiting the possibility to detect small flaws. The typical defects present in composite materials are: delamination, cracks, fibre-matrix debonding and fibres fractures [6, 12–15]. Delamination is probably the most investigated failure mode in composite material laminates [1, 4, 5, 16]. During UT NDT of a composite part, the presence of an extended delamination corresponds to a UT waveform with a reduction of the back echo amplitude together with the appearance of a defect echo located at the delamination depth. Other smaller defects such as voids and inclusions cause a loss of the UT back echo amplitude and/or can be weakly reflected [38, 39]. Flaws (e.g. delamination) lying parallel to the surface of the part subjected to UT inspection can be easily detected utilising normal incidence probes, whereas defects (e.g. cracks and fibre fractures) lying perpendicular to the surface are difficult to detect due to their small reflecting surface (this problem can be solved using angle-beam transducers) [40].

By employing UT through-transmission or pulse-echo techniques, it is possible to locate and size the defects based on the measurements of UT signal amplitude and/or time-of-flight.

The pulse-echo technique allows to characterise the matrix material proprieties (volume fraction, moisture content and porosity) of a composite by evaluating the UT velocity and/or attenuation. Knowing the composite thickness, the attenuation coefficient can be evaluated by measuring the amplitude reduction of the multiple back echoes, and the UT velocity by determining the time spacing between them.

A limitation of UT inspection consists of the difficulty to identify defects located very close to the front surface of the part (known as “dead zone”) where the pulse length is approximately equal to the time period. This problem can be limited by using shorter pulses or immersion testing procedures. The anisotropic and inhomogeneous properties of composite laminates cause high attenuation of the UT waves, internal UT reflections and UT velocity variations due to the presence of different materials (fibres and matrix) and interfaces (fibre-matrix and inter-ply interfaces).

4. Applications

In the last several years, numerous studies were carried out on the application of UT NDT for defect detection in low-velocity impacted composite material laminates.

In 1998, the estimation of impact induced damage under low-velocity impact (impact energy: from 3 to 30 J) in carbon fibre reinforced polymer (CFRP) laminates was investigated in [41] through UT C-scans using the pulse-echo immersion method. Delamination areas were accurately quantified by processing the UT image data and the correlation between impact energy and delamination extension was established.

In [42], an UT NDT system for delamination evaluation in CFRP, glass fibre reinforced plastic (GFRP) and aramid fibre reinforced plastic (AFRP) laminates subjected to low-velocity impact tests (impact energy: 2, 3, 5 J) is described. The UT NDT analysis was performed using two different probes (5 and 15 MHz) to evaluate the influence of frequency on the reliable evaluation of delamination in these composites. The results confirmed the NDT system capabilities in terms of damage detection, location and evaluation.

In [40], the authors demonstrated that a combination of normal and oblique incidence pulse-echo UT techniques provide highly detailed volumetric images of the damage (matrix cracks and delaminations) induced in composite laminates by low-velocity and low-energy impacts. The tested specimens (quasi-isotropic carbon/polyetheretherketone (PEEK) laminates) were immersed in water and scanned at normal (to detect delaminations) and oblique (to identify matrix cracks) incidence using a focussed broadband transducer (3.2 mm diameter, 18 mm focal length) with a centre frequency of 22 MHz.

A comparative analysis of two different NDT techniques, UT air-coupled C-scan and X-ray radiography, applied to thin carbon/epoxy composite laminates, utilised in naval structures, for the detection of low-energy impact damage was carried out by [43]. The damage area was identified by the two NDT techniques but the UT inspection provided for an easier, faster and more accurate damage characterisation.

In [44], the response of CFRP laminates with different stacking sequences (unidirectional, cross-ply, quasi-isotropic and woven laminates) at low impact velocity and under low-temperature

conditions was examined. Low-velocity impact tests at different temperatures were carried out using an impact energy range from 1 to 13 J. After the impact tests, the damage extension was measured by UT C-scan inspection and the damage mechanisms were studied by optical and scanning electron microscopy. The results showed the influence of temperature, ply reinforcement architecture and stacking sequence on the mechanical behaviour of the CFRP laminates subjected to low-velocity impulsive loads.

A multi-functional non-linear UT testing approach was presented in [45] for in-situ and ex-situ detection of diverse defects (micro-cracking, delamination and disbonding) generated by different damage inducing loads (stress, impact and heat) in CFRP materials and structures for aeronautical applications. The impact tests were conducted using several impact loadings ranging from 4 to 69 J impact energy. The applied UT methodology proved to be a useful tool for the identification of damage for impact energy below 30 J where the visual evidence of damage is lacking.

The effect of temperature on low-velocity impact resistance properties and post-impact flexural performance of CFRP laminates was studied in [46] using UT C-scan and micro-focus X-ray computed tomography. A correlation between the impact temperature and the damage area was validated by the results obtained with the two NDT techniques.

A sparse digital signal model was presented in [47] as an efficient model for the estimation of UT measurements obtained from multi-layered composites. A CFRP laminate with stacking sequence $[0/90]_{45}$ was impacted in a drop weight tower with 3.8 J impact energy. The laminate was excited by a low-frequency UT sine-burst with central frequency 5 MHz. The UT response signals were utilised for the validation of the developed digital signal model in order to obtain the damage identification. In [48], a multi-level Bayesian method was utilised to identify the through-the-thickness position and the effective mechanical properties of the damaged layers in the same composite laminates using through-transmission UT measurements.

In [49], the authors experimentally tested three composite structures with barely visible impact (BVI) damage and delaminations, using different NDT techniques including UT scanning, piezoelectric sensing, thermography and vibration-based inspection in order to analyse their applicability in the environmental conditions of aircraft elements inspection. The applied UT technique provided a detailed damage evaluation in terms of damage depth, size and location.

Infrared thermography and phased array UT techniques were employed in [50] to detect the impact damage in CFRP composites. Three values of impact energy (18, 29 and 39 J) were chosen for the tests. Both NDT methods presented advantages and limitations. Thermography is fast in detecting the impact damage over large panels, but it is affected by loss of contrast in case of deep defects. The UT technique is more effective in the estimation of thickness and in the inspection of thick parts, but it can be applied only over smooth surfaces and requires a coupling medium.

A laser-ultrasound (LU) scanner was used in [51] to obtain high-quality images of damage in CFRP composites subjected to low-velocity impact with energies 25 and 50 J. X-ray tomograms were also carried out for comparison with the results of the LU study. The high-speed and high-resolution LU scanning method proved to be efficient for in-situ non-contact imaging of the internal materials structure with resolution higher than 1 ply.

In [52], the response to repeated low-velocity impacts was studied for two types of hybrid laminates made of metal and composite layers specifically designed for aircraft structural applications. The damage was evaluated using visual inspection and UT C-scan procedures. Three categories of impact damage were observed: visible deformation without internal or external damage, visible internal damage (C-scan) without external damage and visible internal and external damages.

An UT technique was used in [53] to investigate the delamination caused by low-velocity impact tests on poly(lactic acid)/jute woven fabric composite laminates obtained by conventional film stacking and compression moulding techniques. Square specimens, 100×100 mm, were impacted in a falling dart test machine using 5 impact energy values: 2, 5, 10, 12 and 15 J. Delamination damage was evaluated through an UT technique employing a linear phased array probe. The delaminated area was correlated with both the impact energy and the measured indentation depth. The results allowed to identify a threshold energy value beyond which internal damage was detected. Moreover, a linear relationship between delaminated area, energy and indentation depth was found.

A delamination prediction method for composite laminates, utilised for application in unmanned aerial vehicles, subjected to low-energy impact was presented in [54]. UT C-scan tests were carried out with UT beam propagation direction from the bottom laminate surface to the top laminate surface that received the impact. Numerical models were built to simulate the delamination behaviour of the composite laminates, showing a good correlation with the experimental UT results. Delamination prediction can contribute to the evaluation of composite residual strength and the optimization of aircraft structures.

In [55], an UT NDT system was utilised to carry out the metrological characterisation of quadriaxial non-crimp fabric (NCF) CFRP composite laminates subjected to low-velocity impact. The scopes of the UT inspection were thickness estimation, stacking sequence and fibre orientation verification, and composite quality assessment in terms of impact damage development within the whole material volume. The same UT NDT system was considered in [33, 55, 56] for diverse UT testing procedures. **Figure 9** illustrates the specially designed hardware and custom-made software of the UT system operating as follows: the UT oscillator/detector excites the piezoelectric immersion UT probe which is displaced by a 6-axis robotic arm. After interacting with the tested material, the reflected UT pulses return to the oscillator/detector which forwards them to a digital oscilloscope for visualisation and digitisation of the UT waveforms. The digitised UT waveforms are then transferred to a PC where a custom-made software code provides for UT waveform signal storage and analysis.

Low-velocity impact tests were performed on rectangular composite specimens under a falling weight machine using a cylindrical indenter with hemispherical nose at different impact energies: 9, 12, 16, 20, 25, 30 and 40 J.

After impact testing, pulse-echo immersion FV-UT scanning was carried out on the impacted specimens with a focused high-frequency transducer (15 MHz) over a 110×155 mm area with scan step 1 mm. The delaminated area was measured through UT image processing. In **Figures 10–12**, four UT images of the impacted quadriaxial laminates are reported for

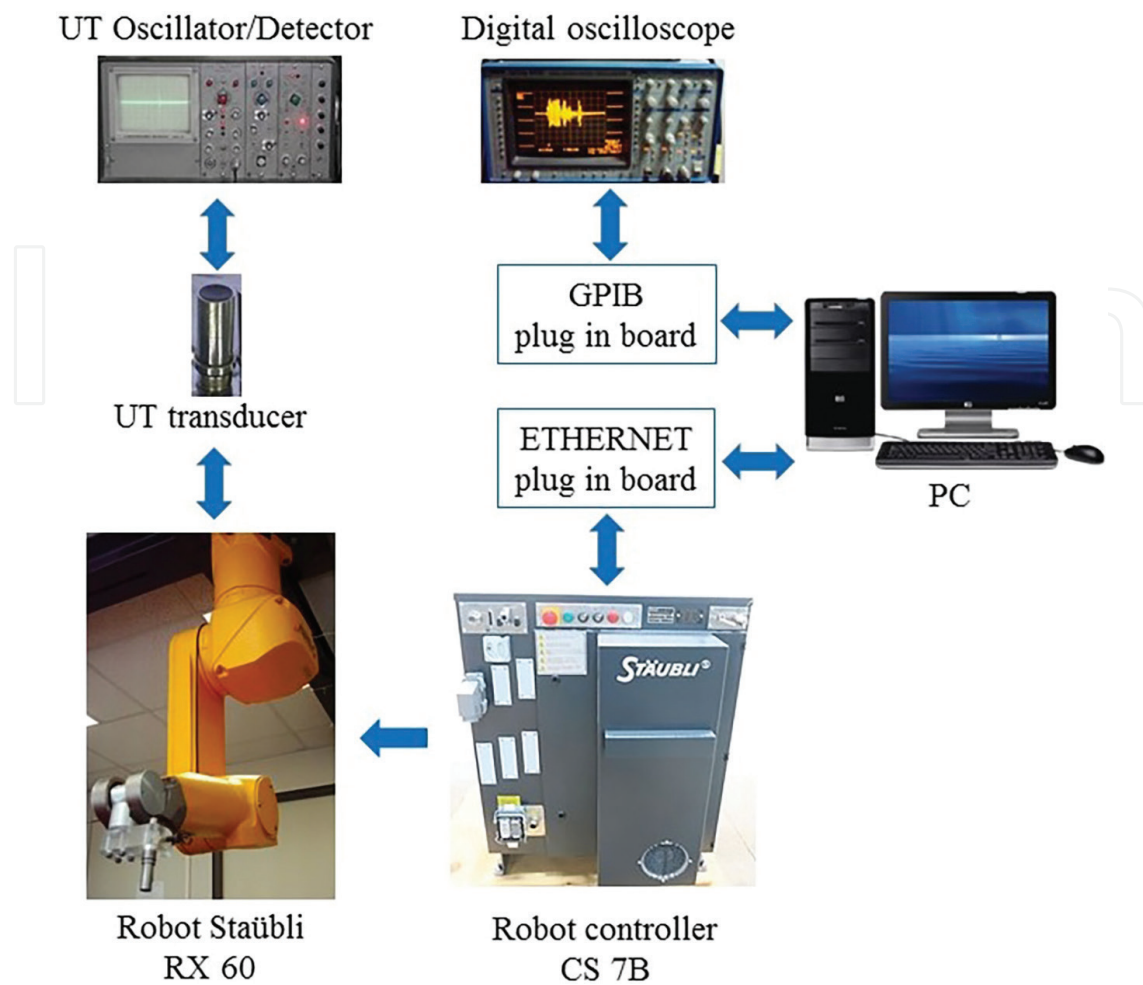


Figure 9. Specially designed UT NDT system.

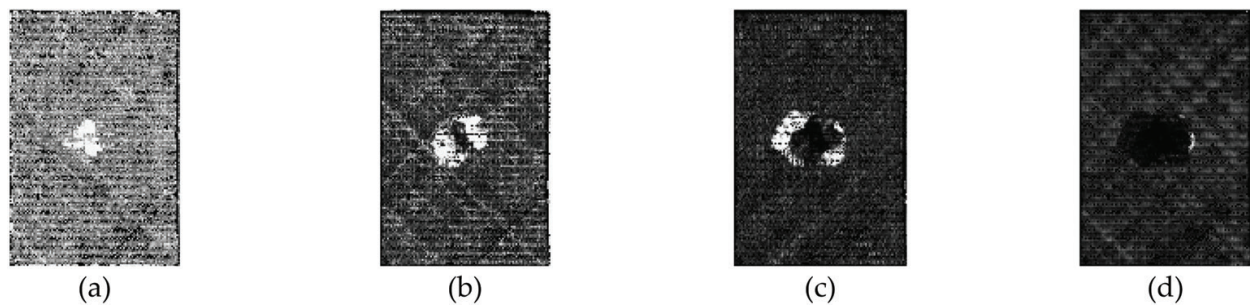


Figure 10. Four UT images for low-energy (9 J) impacted NCF laminate. Each image reports the internal structure of 1 mm thickness from upper (a) to lower laminate surface (d).

drop weight low-velocity impact tests with energy 9, 20 and 40 J, respectively. Each of the four images represents the internal structure of 1/4 (i.e. 1 mm) of the NCF laminate thickness starting from the upper surface (first image on the left) down to the opposite lower surface (last image on the right). In particular, in every figure, image (a) represents the surface damage, images (b) and (c) the internal damage and image (d) the in-plane projection of the total

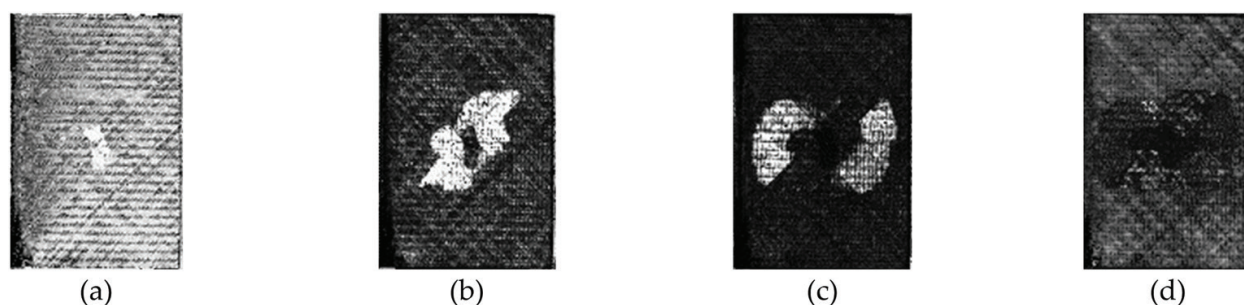


Figure 11. Four UT images for medium energy (20 J) impacted NCF laminate. Each image reports the internal structure of 1 mm thickness from upper (a) to lower laminate surface (d).

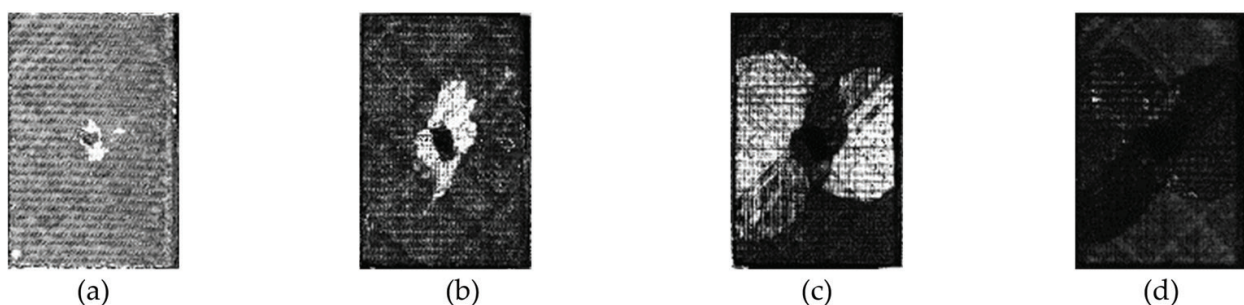


Figure 12. Four UT images for high energy (40 J) impacted NCF laminate. Each image reports the internal structure of 1 mm thickness from upper (a) to lower laminate surface (d).

internal damage. The analysis of the UT images shows that: (i) the impact damage develops differently at interfaces between layers characterised by diverse fibre orientations; (ii) the delamination area increases with rising distance (depth) from the impact surface as well as with growing impact energy and (iii) the delamination outline exhibits the well-known hat-shaped configuration [20]. The UT analysis also reveals the absence of delamination in a small zone directly below the impact surface contact point.

5. Conclusions

In low-velocity impacted composite materials, damages due to this type of loading usually develop inside the material structure and are difficult to detect. Delamination, arising from dynamic loading, is seemingly the most investigated impact failure mode due to its high criticality. However, other damage types such as matrix cracking, fibre-matrix debonding and fibre breakage can also occur due to impact loads. These damage mechanisms can interact with each other and lead to considerable reduction of the load-carrying capability of composite structures. Thus, the thorough material damage characterisation is essential to assess the impact damage criticality. This chapter focussed on the non-destructive characterisation and assessment of low-velocity impact damage in composite material laminates through ultrasonic testing and inspection. A general description of low-velocity impact damage generation in composite materials was presented. Ultrasonic testing methodologies for composite

materials were illustrated and compared in terms of accuracy, resolution and performance. Applications were presented and discussed for industrial areas where composite materials usage is highly relevant.

Author details

Tiziana Segreto^{1,2*}, Roberto Teti^{1,3} and Valentina Lopresto³

*Address all correspondence to: tsegreto@unina.it

1 Fraunhofer Joint Laboratory of Excellence on Advanced Production Technology (Fh-J_LEAPT UniNaples), Naples, Italy

2 Department of Industrial Engineering, University of Naples Federico II, Naples, Italy

3 Department of Chemical, Materials and Industrial Production Engineering, University of Naples Federico II, Naples, Italy

References

- [1] Hong S, Liu D. On the relationship between impact energy and delamination area. *Experimental Mechanics*. 1989;115-120
- [2] Cairns DS, Minuet PJ, Abdallah MG. Theoretical and experimental response of composite laminates with delaminations loaded in compression. *Composite Structures*. 1993;25:113-120
- [3] Choi HY, Chang FK. A model for predicting damage in graphite/epoxy laminated composites resulting from low-velocity point impact. *Journal of Composite Materials*. 1992;26(14):2134
- [4] Liu S, Kutlu Z, Chang FK. Matrix cracking and delamination propagation in laminated composites subjected to transversely concentrated loading. *Journal of Composite Materials*. 1993;27(5):436
- [5] Stout MG, Koss DA, Liu C, Idasetima J. Damage development in carbon/epoxy laminates under quasi-static and dynamic loading. *Composites Science and Technology*. 1999;59:2339-2350
- [6] Liu S. Quasi impact damage initiation and growth of thick-section and toughened composite materials. *International Journal of Solids and Structures*. 1994;31(22):3079-3098
- [7] Castellano A, Fraddosio A, Piccioni MD. Ultrasonic goniometric immersion tests for the characterization of fatigue post-LVI damage induced anisotropy superimposed to the constitutive anisotropy of polymer composites. *Composites Part B: Engineering*. 2017;116:122-136

- [8] Gholizadeh S. A review of non-destructive testing methods of composite materials. *Procedia Structural Integrity*. 2016;**1**:50-57. DOI: 10.1016/j.prostr.2016.02.008
- [9] Shull PJ. *Non-Destructive Evaluation: Theory, Techniques, and Applications*. New York: CRC Press, Taylor and Francis Group; 2002
- [10] Cairns DS. Simple elasto-plastic contact laws for composites. *Journal of Reinforced Plastics and Composites*. 1991;**10**(4):423-433
- [11] Bucinell RB, Nuismer RJ, Koury JL. Response of composite plates to quasi-static impact events. *ASTM STP 1110*, TK O'Brien, ed.; 1991. pp. 528-549
- [12] Abrate S. Impact on laminated composites: Recent advances. *Applied Mechanics Reviews*. 1994;**47**(11):517-544
- [13] Hull D, Shi YB. Damage mechanism characterisation in composite damage tolerance investigations. *Composite Structures*. 1993:99-120
- [14] Hitchen SA, Kemp RMJ. The effect of stacking sequence on impact damage in a carbon fibre/epoxy composite. *Composites*. 1995;**26**:207-214
- [15] Richardson MOW, Wisheart MJ. Review of low-velocity impact properties of composite materials. *Composites Part A Applied Science and Manufacturing*. 1996;**27A**:1123-1131
- [16] Caprino G. Residual strength prediction of impacted CFRP laminates. *Journal of Composite Materials*. 1984;**18**:508-518
- [17] Cantwell WJ, Morton J. The impact resistance of composite materials - a review. *Composites*. 1991;**22**(5):347-362
- [18] Kim JK, Mackay DB, Mai YW. Drop-weight impact damage tolerance of CFRP with rubber-modified epoxy matrix. *Composites*. 1993;**24**(6):485-494
- [19] Choi HY, Downs RJ, Chang FK. A new approach toward understanding damage mechanisms and mechanics of laminated composites due to low velocity impact: Part I-experiments. *Journal of Composite Materials*. 1991;**25**:992-1011
- [20] Abrate S. *Impact on Composite Structures*. Cambridge: Cambridge University Press;
- [21] Choi HY, Chang FK. A model for predicting damage in graphite/epoxy laminated composites resulting from low-velocity point impact. *Journal of Composite Materials*. 1992;**26**(14):2134-2169
- [22] Caprino G, Lopresto V. The significance of indentation in the inspection of CFRP panels damaged by low-velocity impact. *Composites Science and Technology*. 2000;**60**:1003-1012
- [23] Cantwell WJ, Morton J. Impact perforation of carbon fibre reinforced plastics. *Composites Science and Technology*. 1990;**38**:119-141
- [24] Caprino G, Lopresto V, Scarponi C, Briotti G. Influence of material thickness on the response of carbon-fabric/epoxy panels to low-velocity impact. *Composites Science and Technology*. 1999;**59**:2279-2286

- [25] Caprino G, Langella A, Lopresto V. Elastic behaviour of circular composite plates transversely loaded at the Centre. *Composites Part A Applied Science and Manufacturing*. 2002;**33**:1191-1197
- [26] Sjoblom PO, Hartness TM, Cordell TM. On low-velocity impact testing of composite materials. *Journal of Composite Materials*. 1998;**22**(1):30-52
- [27] Herup EJ, Palazotto AN. Low-velocity impact damage initiation in graphite/epoxy/Nomex honeycomb-sandwich plates. *Composites Science and Technology*. 1997;**57**(12):282-289
- [28] Hashin Z. Failure criteria of unidirectional fiber composites. *Journal of Applied Mechanics*. 1975;**47**:329
- [29] Graff KF. A history of ultrasonics. In: *Physical Acoustics*. Vol. XV. NY: Academic Press;
- [30] Sokolov S. *Phys. Z.* 1935;**36**(142) and *Techn. Physic USSR* 1935;**2**:522
- [31] Firestone FA. Patent n. US 2280226A. Flaw Detecting Device and Measuring Instrument
- [32] McNulty JF. Patent n. US3260105A. Ultrasonic Testing Apparatus and Method; 1962
- [33] Segreto T, Caggiano A, Teti R. Quality assurance of brazed copper plates through advanced ultrasonic NDE. *Procedia CIRP*. 2016;**55**:194-199. DOI: 10.1016/j.procir.2016.08.048
- [34] Blitz J, Simpson G. *Ultrasonic Methods of Non-Destructive Testing*. London, UK: Chapman & Hall; 1995
- [35] ASTM. E494-15 Standard Practice for Measuring Ultrasonic Velocity in Materials. PA: West Conshohocken; 2015. DOI: 10.1520/E0494-15
- [36] Krautkrämer J, Krautkrämer H. *Ultrasonic Testing of Materials*. Berlin Heidelberg: Springer-Verlag; 1990. 677 p. DOI: 10.1007/978-3-662-10680-8
- [37] Chaplin R. *Industrial Ultrasonic Inspection: Levels 1 and 2*. Canada: Friesen Press; 2017. 292 p
- [38] Teti R. Ultrasonic identification and measurement of defects in composite material laminates. *CIRP Annals*. 1990;**39**(1):527-530
- [39] Summerscales J. *Non-Destructive Testing of Fibre-Reinforced Plastics Composites*. Vol. 2. Springer Science & Business Media; 1990. 493 p
- [40] Aymerich F, Meili S. Ultrasonic evaluation of matrix damage in impacted composite laminates. *Composites Part B: Engineering*. 2000;**31**(1):1-6. DOI: 10.1016/S1359-8368(99)00067
- [41] Hosur MV, Murthy CRL, Ramamurthy TS, Shet A. Estimation of impact-induced damage in CFRR laminates through ultrasonic imaging. *NDT and E International*. 1998;**31**(5):359-374
- [42] Scarponi C, Briotti G. Ultrasonic technique for the evaluation of delaminations on CFRP, GFRP, KFRP composite materials. *Composites Part B: Engineering*. 2000;**31**(3):237-243
- [43] Imielińska K, Castaings M, Wojtyra R, Haras J, LeClezio E, Hosten B. Air-coupled ultrasonic C-scan technique in impact response testing of carbon fibre and hybrid: Glass,

- carbon and Kevlar/epoxy composites. *Journal of Materials Processing Technology*. 2004;**157-158**:513-522
- [44] Gómez-del Río T, Zaer R, Barbero E, Navarro C. Damage in CFRPs due to low velocity impact at low temperature. *Composites Part B: Engineering*. 2005;**36**(1):41-50
- [45] Armitage PR, Wright CD. Design, development and testing of multi-functional non-linear ultrasonic instrumentation for the detection of defects and damage in CFRP materials and structures. *Composites Science and Technology*. 2013;**87**:149-156
- [46] Suvarna R, Arumugam V, Bull DJ, Chambers AR, Santulli C. Effect of temperature on low velocity impact damage and post-impact flexural strength of CFRP assessed using ultrasonic C-scan and micro-focus computed tomography. *Composites Part B: Engineering*. 2014;**66**:58-64. DOI: 10.1016/j.compositesb.2014.04.028
- [47] Bochud N, Gomez AM, Rus G, Peinado AM. A sparse digital signal model for ultrasonic nondestructive evaluation of layered materials. *Ultrasonics*. 2015;**62**:160-173
- [48] Chiachío J, Bochud N, Chiachío M, Cantero S, Rus G. A multilevel Bayesian method for ultrasound-based damage identification in composite laminates. *Mechanical Systems and Signal Processing*. 2017;**88**:462-477. DOI: 10.1016/j.ymssp.2016.09.035
- [49] Katunin A, Dragan K, Dziendzikowski M. Damage identification in aircraft composite structures: A case study using various non-destructive testing techniques. *Composite Structures*. 2015;**127**:1-9. DOI: 10.1016/j.compstruct.2015.02.080
- [50] Meola C, Boccardi S, Carlomagno GM, Boffa ND, Monaco E, Ricci F. Nondestructive evaluation of carbon fibre reinforced composites with infrared thermography and ultrasonics. *Composite Structures*. 2015;**134**:845-853. DOI: 10.1016/j.compstruct.2015.08.119
- [51] Pelivanov I, Ambroziński L, Khomenko A, Koricho EG, Cloud GL, Haq M, et al. High resolution imaging of impacted CFRP composites with a fiber-optic laser-ultrasound scanner. *Photoacoustics*. 2016;**4**(2):55-64. DOI: 10.1016/j.pacs.2016.05.002
- [52] Sadighi M, Tooski MY, Alderliesten RC. An experimental study on the low velocity impact resistance of fibre metal laminates under successive impacts with reduced energies. *Aerospace Science and Technology*. 2017;**67**:54-61. DOI: 10.1016/j.ast.2017.03.042
- [53] Papa I, Lopresto V, Simeoli G, Langella A, Russo P. Ultrasonic damage investigation on woven jute/poly (lactic acid) composites subjected to low velocity impact. *Composites Part B: Engineering*. 2017;**115**:282-288. DOI: 10.1016/j.compositesb.2016.09.076
- [54] Wang HR, Long SC, Zhang XQ, Yao XH. Study on the delamination behavior of thick composite laminates under low-energy impact. *Composite Structures*. 2018;**184**:461-473
- [55] Segreto T, Bottillo A, Teti R. Advanced ultrasonic non-destructive evaluation for metrological analysis and quality assessment of impact damaged non-crimp fabric composites. *Procedia CIRP*. 2016;**41**:1055-1060. DOI: 10.1016/j.procir.2015.12.125
- [56] Segreto T, Bottillo A, Caggiano A, Teti R, Ricci F. Full-volume ultrasonic technique for 3D thickness reconstruction of CFRP aeronautical components. *Procedia CIRP*. 2018;**67**:434-439. DOI: 10.1016/j.procir.2017.12.238